Carbon 129 (2018) 374–379

Contents lists available at ScienceDirect

Carbon

journal homepage: www.elsevier.com/locate/carbon

Highly efficient water desalination in carbon nanocones

Wen Li [a, b, 1], Wensen Wang [a, 1], Yingnan Zhang [a], Youguo Yan [a], Petr Král [b, c, d, *], Jun Zhang [a, **]

[a] College of Science, China University of Petroleum (East China), Qingdao, Shandong 266580, People's Republic of China
[b] Department of Chemistry, University of Illinois at Chicago, Chicago, IL 60607, United States
[c] Department of Physics, University of Illinois at Chicago, Chicago, IL 60607, United States
[d] Department of Biopharmaceutical Sciences, University of Illinois at Chicago, Chicago, IL 60607, United States

ARTICLE INFO

Article history:
Received 14 September 2017
Received in revised form
21 November 2017
Accepted 9 December 2017
Available online 12 December 2017

ABSTRACT

Inspired by the highly efficient water transport presented in hourglass-shaped aquaporin channels, molecular dynamics simulations were conducted to study water desalination in carbon nanocones (CNCs). Their desalination performance (salt rejection, water flow) depends on the cone size, angle, and flow direction (nonequilibrium). Free energy calculations reveal that ultrasmall CNCs with apex angles of 19.2° provide the best desalination performance, since they contain relatively ordered water structures, providing high water flows, but have a high ion rejection rate. The desalination performance observed in these CNCs is better than in nanoporous graphene and MoS_2 monolayers.

1. Introduction

Freshwater shortage is becoming a worldwide problem due to a global climate change, growing population, and increasing industrial and agricultural consumptions [1,2]. Seawater covers 70% of earth surface [3] and could provide a plentiful resource of freshwater, if efficient desalination methods are developed. However, due to a large energy consumption and trade-off between water permeability and salt rejection rate [4], the desalination efficiency is unsatisfactory in currently used reverse osmosis (RO) methods [5].

In carbon nanotubes (CNT) [6,7], water can flow almost without friction, since its flow rate is 4–5 orders of magnitude larger than predicted by a classical fluid-flow theory [8]. Efficient desalination membranes have been constructed using aligned ultranarrow CNTs [9–11]. Efforts were also made to prepare highly permeable and selective ultrathin membranes based on nanoporous graphene [12–19], graphyne [20,21], molybdenum disulfide (MoS_2) [22,23], and other 2D materials [24–26]. Many of these nanoporous materials have a large potential in water desalination, since they have a high water permeability and salt rejection rates.

Nature provides great inspiration by its design principles and solutions. For example, biological channels in cell membranes are highly selective, permeable, and environmentally sensitive [27–30], which is difficult to achieve simultaneously in synthetic nanochannels [31–35]. Due to a high water permeability and selectivity, aquaporins (AQPs) play a crucial role in the passage of water across cell membranes [36]. AQPs have an hourglass-shaped channel structure [37,38], in which the narrow neck is responsible for a high water selectivity, and the conical entrance for a high water permeability (reduced hydrodynamic entrance resistance). In principle, similar conical structures could enhance fluidic flow in synthetic nanochannels [38–43]. Inspired by the nearly frictionless water flow in CNTs and the highly permeable and selective water flow in conical AQPs, we assume that a high desalination performance can be achieved in carbon nanocones (CNCs). Here, we perform molecular dynamics (MD) simulations to examine this possibility.

2. Models

Fig. 1 shows the studied model system. A fixed CNC of a 2 nm length is held between two fixed graphene sheets with pores matching the CNC channel. Two more (rigid) graphene slabs were used to maintain constant pressures at the left and right regions of the system. When the desalination took part from the base (tip) to the tip (base) sides, salt water (0.5 mol/L NaCl) was left at the left (right) of the CNC channel (high pressure region), and pure water

* Corresponding author. Department of Chemistry, University of Illinois at Chicago, Chicago, IL 60607, United States.
** Corresponding author. College of Science, China University of Petroleum (East China), Qingdao, Shandong 266580, People's Republic of China.
E-mail addresses: pkral@uic.edu (P. Král), zhangjun.upc@gmail.com (J. Zhang).
[1] Wen Li and Wensen Wang contributed equally.

https://doi.org/10.1016/j.carbon.2017.12.039
0008-6223/

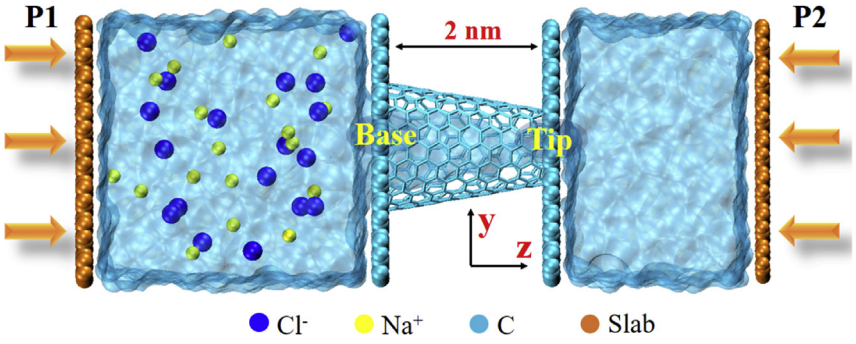

Fig. 1. The constructed system used in this work. Water was shown as transparent cyan. (A colour version of this figure can be viewed online.)

was put at the right (left) of the CNC channel (low pressure region -0.1 MPa). Periodic boundary conditions were applied in the X and Y directions.

The atomistic MD simulations were performed using LAMMPS [44] and a modified CHARMM force field. Water was described by a TIP3P model [45], where the SHAKE algorithm was used to keep the rigidity of water molecules. The ion-ion Lennard-Jones (LJ) parameters were obtained from literature [46], the carbon-carbon (sp^2 carbons) LJ parameters were $\sigma_{cc} = 0.33997$ nm and $\varepsilon_{cc} = 0.0859$ kcal/mol. Other LJ parameters were obtained using the Lorentz-Berthelot combining rules [47], as summarized in Table S1. The van der Waals (vdW) coupling was calculated with a cutoff of 12 Å and the particle-Particle-Particle-Mesh (PPPM) method was used for the calculation of long-range electrostatic interactions. The MD simulations were conducted in NVT ensemble at 298 K, with a time step of 1 fs, and the data were collected every 1 ps. The total simulation time of each system was 10 ns.

3. Results and discussion

Depending on the number of pentagons at the CNC apex [48], five symmetric CNCs exist with apex angles of 112.9°, 83.6°, 60.0°, 38.9° and 19.2°. Here, the CNCs tips were cut (Fig. 1) and their accessible pore areas are shown in Fig. S1 and described in Table S1. The tip pore areas in cut CNCs with apex angles of 19.2°, 38.9° and 60°, ranging from 19.30 to 19.37 $Å^2$, are similar to 19.29 $Å^2$ for (6, 6) CNT and 19.38 $Å^2$ for a nanoporous graphene (GN), which could both be used for desalination [49]. All the studied models are shown in Fig. S2.

First, we studied desalination under different hydrostatic pressures in a cut CNC with an apex angle of 19.2° (CNC-19.2°) and a tip pore area of 19.30 $Å^2$, as shown in Fig. S3. An approximately linear relationship between the pressure and water flux, but a full ion rejection, were observed. Therefore, in order to get enough statistics in a limited simulation time, a relatively large hydrostatic pressure of 100 MPa was adopted in the following simulations. Using these conditions, we examine the desalination performance (water flux and ion rejection) of systems shown in Fig. S2.

Water flux. Fig. S4 shows a time-dependent flow of filtered water at hydrostatic pressure of 100 MPa from the base (tip) to tip (base) sides for systems shown in Fig. S2. The calculated water fluxes (slopes of the curves in Fig. S4) are shown in Fig. 2, and the error bar was given based on three separated simulations. In the (6,6) CNT, a water flux of ~15 #/ns passes under 100 MPa pressure, in agreement with previous studies [49]. Three observations also could be done from these simulations: (1) the CNC systems have higher water flux than the CNT and GN systems, (2) the flow rate depends on the CNC orientation (higher water flux emerges from the base to tip side) and (3) the water flux increases with the decreasing CNC apex angles and reaches a maximum at 19.2°.

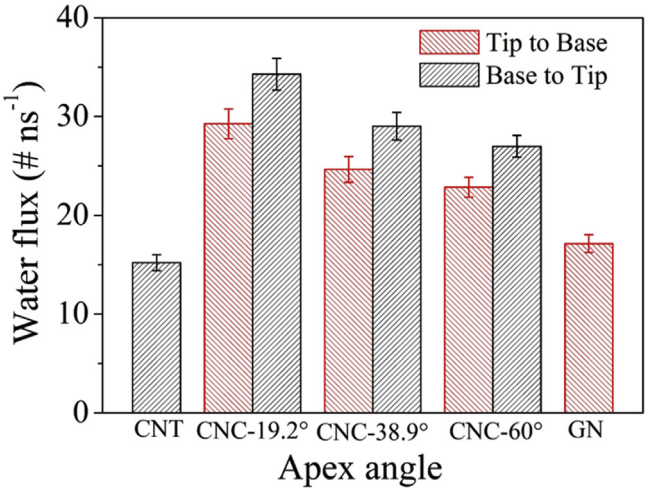

Fig. 2. Water flux from the base (tip) to tip (base) sides of CNCs with different apex angles. (A colour version of this figure can be viewed online.)

To understand the (1) point, the potential of mean forces (PMFs) of water was calculated in these channels to estimate the energy barriers for water transport (see SI for the detailed PMF calculation). Fig. 3a shows that in CNCs with larger angles the energy barrier decreases at the base side (cone diameter increases) but slightly increases at the tip side (cone diameter stays the same), where it eventually approaches the barrier presented in GN with the same diameter as the CNCs tips. This could explain why the smallest water flux is present in GN. Similarly, in the chosen CNT, the energy barrier is on average larger than in all the other systems, which gives the weakest water flux. To further understand the larger water flux in CNC channels quantitatively, we calculated the average axial velocity of water molecules passing through the CNT, GN and the tip side of the CNC channels (Table S2). We can see water molecules in CNC channels have larger velocities, which also indicate their larger water flux than that of CNT or GN systems.

When water flows in CNCs from the base to the tip sides, the gently increasing energy barriers permits a lot of water to enter, which contributes to their higher water flux. Similarly, when water flows in the opposite way, it can easily diffuse out of the channels, which also gives relatively larger flows. The larger base side pores in CNCs and the corresponding higher likelihood of collecting water from the solution under pressure (Fig. 3b) are responsible for higher water fluxes from the base to the tip sides, which explains the (2) point. However, this feature disappears at small pressures, since close to equilibrium both passage rates should be the same,